Chapter 5

Cell Cycle Resolved Measurements of Poly(ADP-Ribose) Formation and DNA Damage Signaling by Quantitative Image-Based Cytometry

Jone Michelena and Matthias Altmeyer

Abstract

Formation of poly(ADP-ribose) (PAR) marks intracellular stress signaling and is notably induced upon DNA damage. PAR polymerases (PARPs) catalyze PAR synthesis upon genotoxic stress and thereby recruit multiple proteins to damaged chromatin. PAR induction is transient and antagonized by the action of PAR glycohydrolase (PARG). Given that poly(ADP-ribosyl)ation (PARylation) is involved in genome integrity maintenance and other vital cellular functions, but also in light of the recent approval of PARP inhibitors for cancer treatments, reliable measurements of intracellular PAR formation have gained importance. Here we provide a detailed protocol for PAR measurements by quantitative image-based cytometry. This technique combines the high spatial resolution of single-cell microscopy with the advantages of cell population measurements through automated high-content imaging. Such upscaling of immunofluorescence-based PAR detection not only increases the robustness of the measurements through averaging across large cell populations but also allows for the discrimination of subpopulations and thus enables multivariate measurements of PAR levels and DNA damage signaling. We illustrate how this technique can be used to assess the dynamics of the cellular response to oxidative damage as well as to PARP inhibitor-induced genotoxicity in a cell cycle resolved manner. Due to the possibility to use any automated microscope for quantitative image-based cytometry, the presented method has widespread applicability in the area of PARP biology and beyond.

Key words Poly(ADP-ribose) (PAR), PARP1, ARTD1, PARP inhibitors, Olaparib, DNA damage, Cell cycle, Cytometry, High-content microscopy, Quantitative single-cell analyses

1 Introduction

PARylation is a highly dynamic posttranslational protein modification that comprises the attachment of multiple ADP-ribose units derived from nicotinamide adenine dinucleotide (NAD^+) onto target proteins by PARPs, also referred to as ARTDs [1]. PAR chains can range from short oligomers to long and branched polymers, which regulate target protein functions and provide a recruitment platform for PAR-binding proteins [2]. Through dynamic and context-dependent assembly of PAR-binding proteins, PARylation can reorganize

Alexei V. Tulin (ed.), *Poly(ADP-Ribose) Polymerase: Methods and Protocols*, Methods in Molecular Biology, vol. 1608,
DOI 10.1007/978-1-4939-6993-7_5,

cellular architecture and contribute to the formation and maintenance of non-membrane-bound compartments, including transient PAR-dependent protein assemblies at regions where genome integrity is compromised [3, 4]. The growing interest in PAR biology, not least sparked by the clinical promises associated with PARP inhibitors for the treatment of cancers defective in homology-directed DNA repair [5, 6], calls for robust and reliable methods to quantitatively assess cellular PAR formation and to directly relate PAR induction to genome integrity maintenance and cell proliferation. Given that PARylation is not only implicated in maintaining genome stability but also plays important roles in various other cellular contexts [7], the development of unbiased approaches to measure cellular PAR levels and monitor their dynamic changes in response to different stress stimuli has become a pivotal task.

Recent advances in quantitative proteomics and genomics have started to elucidate PAR interactions, identify PAR acceptor sites, and map genomic loci that are preferentially PARylated [8–14]. These approaches typically generate cell population averages from millions of lysed cells. In contrast to these powerful techniques, PAR detection by indirect immunofluorescence represents an inexpensive and easy-to-perform single-cell assay, which benefits from the ever-increasing spatiotemporal resolution associated with improved imaging technologies. Here, we provide a detailed protocol, which, based on automated microscopy and software-assisted image analysis, transforms single-cell PAR measurements into a robust quantitative cell population assay. Consistent with previous work [15], we show how such upscaling of single-cell microscopy allows for image-based cell cycle staging and can thereby reveal subpopulation-specific responses. Comparable to imaging flow cytometry [16], the presented workflow combines the advantages of analyzing thousands of individual cells per condition with the high spatial resolution and light sensitivity of state-of-the-art microscope lenses. While the presented protocol reflects principles of multivariate high-content imaging used in advanced large-scale perturbations screens [17, 18] and faces similar challenges in terms of data visualization and analysis [19], it is equally applicable for dedicated small-scale experiments and can be easily adjusted to address a variety of biological questions [3, 11, 20–23].

Applied to PAR biology and DNA damage signaling, quantitative image-based cytometry represents an informative, robust, and reliable technique to assess dynamic changes in intracellular PAR levels, and it complements existing technologies that currently lack single-cell information and are thus unable to discern subpopulation responses. We illustrate on two examples how quantitative image-based cytometry can provide illuminating insights into PAR biology. First, using oxidative stress as a stimulus, we simultaneously assess the dynamics of PAR induction and time-delayed DNA damage signaling in a cell cycle resolved manner (Fig. 1). Second,

using the FDA-approved PARP inhibitor olaparib, we determine induction of S-phase-specific DNA damage signaling accompanied by a delay in cell cycle progression even upon short-term exposure (Fig. 2). We use these examples to highlight the benefits associated with quantitative high-content single-cell imaging, discuss

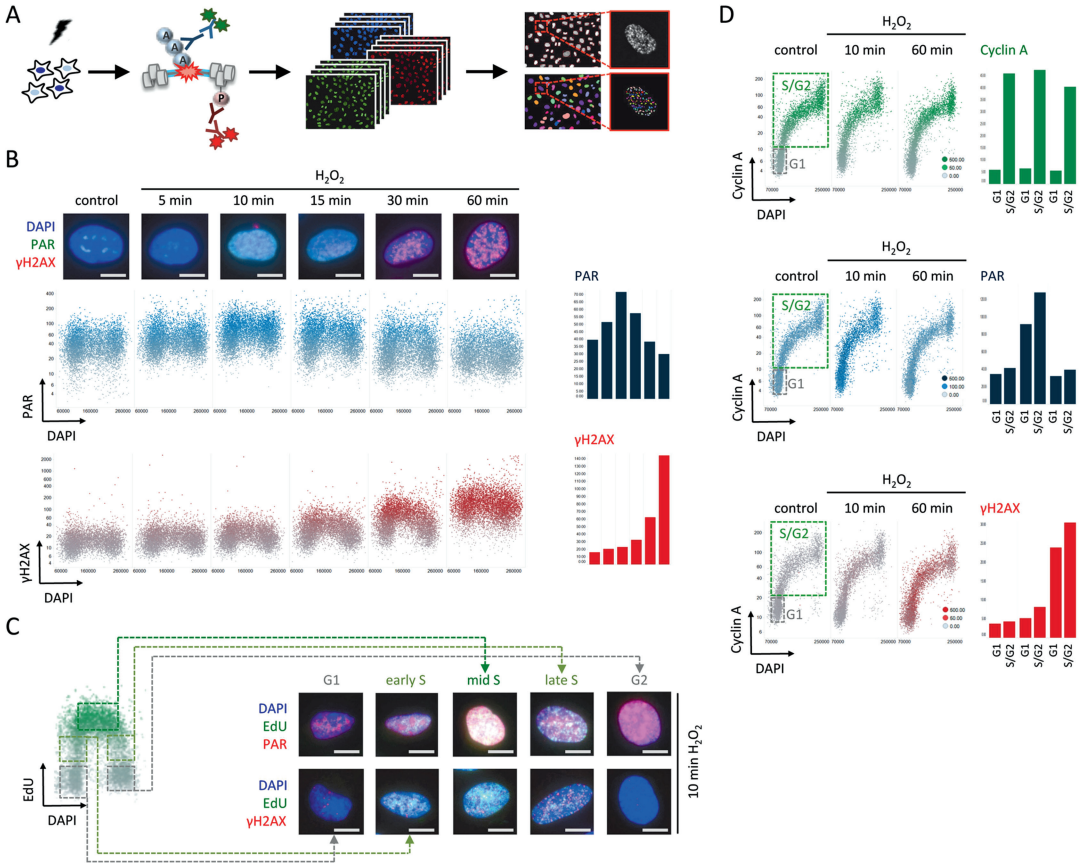

Fig. 1 Quantitative image-based cytometry for cell cycle resolved measurements of PAR formation and DNA damage signaling in response to oxidative damage. (**a**) Schematic overview of the experimental workflow. It comprises treatment of cells, immunofluorescence staining, automated multichannel multi-image acquisition, software-assisted cell segmentation, and image-based feature extraction. A, ADP-ribosylation; P, phosphorylation. (**b**) Asynchronously growing populations of adherent U-2 OS cells were treated for the indicated time-points with 0.1 mM H_2O_2, fixed in 3% formaldehyde, and stained for DNA content (DAPI, blue), PAR (green), and γH2AX (red). Representative images of individual cells are shown. Scatter plots depict single-cell data of more than 5000 cells per condition. Mean PAR, mean γH2AX, and total DAPI intensities per nucleus are shown. Bar charts to the right depict mean cell population averages. (**c**) Cells were pulse-labeled with EdU, treated for 10 min with 0.1 mM H_2O_2, and stained for PAR or γH2AX. The scatter plot depicts single-cell data of more than 5000 cells. Mean EdU and total DAPI intensities per nucleus are shown. Representative images of individual cells in the different cell cycle phases are displayed to the right. **(d)** Cells were treated as indicated with 0.1 mM H_2O_2 and stained for cyclin A and PAR (top and middle panel) or cyclin A and γH2AX (lower panel). Scatter plots depict single-cell data of more than 5000 cells per condition. Mean cyclin A and total DAPI intensities per nucleus are shown. Color code: Cyclin A (top), PAR (middle), and γH2AX (bottom). Bar charts depict cell cycle resolved mean cyclin A (top), PAR (middle), and γH2AX (bottom) levels as cell subpopulation averages. Scale bars: 10 μm

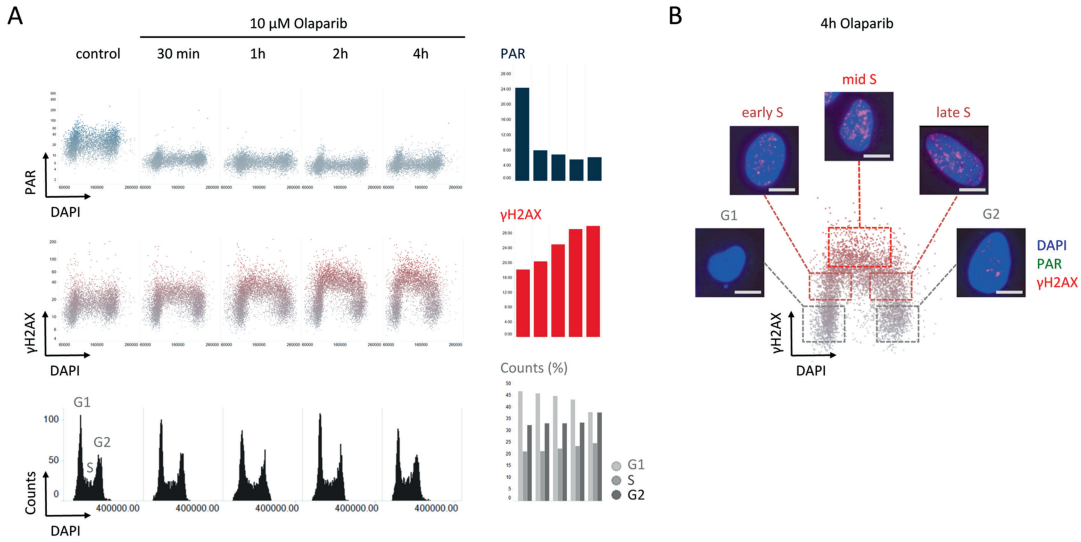

Fig. 2 Quantitative image-based cytometry for cell cycle resolved measurements of PARP inhibitor-induced DNA damage signaling. (**a**) Asynchronously growing populations of U-2 OS cells were treated for the indicated time-points with 10 μM olaparib, fixed in 3% formaldehyde, and stained for DNA content (DAPI), PAR, and γH2AX. Scatter plots depict single-cell data of more than 5000 cells per condition. Mean PAR, mean γH2AX, and total DAPI intensities per nucleus are shown. Bar charts to the right depict mean cell population averages. Also shown are one-dimensional cell cycle profiles based on total DAPI intensities of 5000 cells per condition as well as cell cycle phase distributions to the right. (**b**) Representative images of individual cells from (**a**) in the different cell cycle phases are shown. Scale bars: 10 μm

limitations of this approach, and provide experimental guidelines that can be used to perform similar assays on any automated fluorescence microscope.

2 Materials

2.1 Cell Culture

For standard mammalian cell culture, Dulbecco's modified Eagle's medium (DMEM), fetal calf serum (FCS), and penicillin/streptomycin (P/S) were used. For treatment and labeling of cells, hydrogen peroxide (H_2O_2), PARP inhibitor olaparib, and 5-ethynyl-2′-deoxyuridine (EdU) were used.

2.2 Indirect Immunofluorescence

1. Fixation: 3% formaldehyde in PBS.
2. Permeabilization: 0.2% Triton X-100 in PBS.
3. Blocking solution: Filtered DMEM containing 10% FCS and 0.01% sodium azide.
4. Click-iT EdU Alexa Fluor 488 Imaging Kit (Thermo Fisher Scientific) is used for EdU detection.
5. Primary antibodies: Anti-PAR (Enzo Life Sciences, 1:1000), anti-H2A. X-Phosphorylated (Ser139) (BioLegend, 1:1000), anti-cyclin A2 (Abcam, 1:200; SantaCruz, 1:200).

6. Secondary antibodies: Alexa Fluor 488 goat anti-rabbit (Thermo Fisher Scientific, 1:500), Alexa Fluor 488 goat anti-mouse (Thermo Fisher Scientific, 1:500), Alexa Fluor 647 goat anti-rabbit (Thermo Fisher Scientific, 1:500), Alexa Fluor 647 goat anti-mouse (Thermo Fisher Scientific, 1:500).
7. 4′,6-Diamidino-2-phenylindole dihydrochloride (DAPI): 5 mg/ml stock solution kept at 4 °C for short-term storage and at −20 °C for long-term storage. Protect from light. Prepare 0.5 μg/ml working solution in PBS before use.
8. Mounting media: Mowiol 4.88, Glycerol, and Tris.

2.3 Image Acquisition and Analysis

1. Although image acquisition can be performed manually on any wide-field or confocal fluorescence microscope, multichannel multi-position imaging is best achieved on motorized microscopes equipped with a robust autofocus system. Here, we have used the Olympus ScanR screening system equipped with an inverted motorized Olympus IX83 microscope, a motorized stage, infrared laser-based hardware autofocus (IX3-ZDC), a fast emission filter wheel with single-band emission filters for DAPI, FITC, Cy3, and Cy5, high NA air objectives (4× objective, NA 0.16; 10× objective, NA 0.40; 20× objective, NA 0.75; 40× objective, NA 0.90), and a 12-bit digital monochrome CMOS camera with sensor chip FL-400 (2048 × 2048 pixels of size 6.5 × 6.5 μm). Automated image acquisition employing both hardware and software autofocus was performed using the ScanR acquisition software (Olympus).
2. Image analysis can be performed using a variety of appropriate software packages, which are either commercially available or open source. Here, we have used the ScanR analysis software (Olympus) for image processing, object detection and segmentation, intensity measurements, and gating. Further, we have used the Spotfire data visualization and analytics software (TIBCO) to generate color-coded scatter plots and quantify signal intensities from cell populations and subpopulations.

3 Methods

3.1 Cell Culture Conditions

1. Human U-2 OS osteosarcoma cells are cultured in DMEM supplemented with 10% FCS and 1% P/S at 37 °C with 5% CO_2 in a humidified incubator.
2. To modulate cellular PAR levels, cells are subjected to one of the following treatments: Oxidative stress is induced by 0.1 mM hydrogen peroxide (H_2O_2) treatment (Fig. 1). PARP inhibitor olaparib is used at a final concentration of 10 μM (Fig. 2).

3. To measure DNA synthesis by EdU labeling, U-2 OS cells are pulsed with the nucleoside analog at final concentration of 10 μM for 20 min prior to fixation.

3.2 Indirect Immunofluorescence

1. Cells are seeded onto sterilized 12 mm coverslips placed in 60 mm dishes and grown for 24 h to reach a cell density of 70–90% (*see* **Note 1**).
2. Cells on coverslips are transferred to 24-well plates and subjected to the different treatments for various time periods by replacing the growth medium with medium containing the desired compound (*see* **Note 2**).
3. After treatment, the medium is removed, and cells are washed once with PBS.
4. Cells are fixed with 3% formaldehyde in PBS for 12 min at room temperature. After fixation, the formaldehyde solution is removed, and the cells are washed with PBS. At this point the coverslips can be stored in PBS at 4 °C until staining (*see* **Note 3**).
5. Cell permeabilization is performed by incubation in 0.2% Triton X-100 in PBS for 5 min at room temperature.
6. Cells are washed twice in PBS and incubated in blocking solution for 15 min at room temperature.
7. When combining the staining with an EdU Click-iT reaction, this reaction is performed prior to incubation with the primary antibodies according to the manufacturer's recommendations (Thermo Fisher Scientific). Following the Click-iT reaction, coverslips are washed once with blocking solution (*see* **Note 4**).
8. The blocking solution is removed, and the coverslips are inverted over 35 μl of the desired primary antibody diluted in blocking solution and prepared on a flattened piece of parafilm. Primary antibody incubation is performed for 2 h at room temperature in a humidified chamber (*see* **Note 5**).
9. The coverslips are transferred back to the 24-well dishes and washed three times with PBS.
10. The coverslips are inverted over 35 μl of fluorophore-conjugated secondary antibody diluted in blocking solution and prepared on a flattened piece of parafilm. Secondary antibody incubation is performed for 1 h at room temperature in a humidified, light-protected chamber (*see* **Note 6**).
11. The coverslips are transferred back to the 24-well dishes, washed once with PBS, and the DNA is stained by addition of DAPI solution for 10 min (*see* **Note 7**).
12. The coverslips are washed three times with PBS, dipped into distilled water, placed on tissue paper to dry, and mounted on 5 μl Mowiol-based mounting medium (*see* **Note 8**).

3.3 Automated Microscopy and Image Analysis

1. Multiple images per condition are acquired in an unbiased manner and under non-saturating imaging conditions. The choice of objective and number of acquired images per condition depend on the desired readout and the required image resolution (*see* **Note 9**). While the Olympus ScanR system provides a suitable platform for quantitative image-based cytometry, in principal any automated microscope can be used for multi-image acquisitions (*see* **Note 10**).
2. A moderate dynamic background correction is applied, and nuclei segmentation is performed based on DAPI signals using an intensity threshold-based object detection module to generate masks that identify nuclei as individual objects. This mask is then applied to quantify pixel intensities in the different color channels. Pulsed EdU incorporation, total DAPI levels, and mean intensities of PAR, γH2AX, and cyclin A are measured (*see* **Note 11**). The Olympus ScanR image analysis software enables such image-based feature extraction and intensity quantification; however, various other software packages, including open-source software, allow for similar types of analyses (*see* **Note 12**).
3. The extracted data is imported to the propriety Spotfire data visualization software (TIBCO). Spotfire is used to generate color-coded scatter plots in a flow cytometry-like fashion and to quantify percentages and cell (sub)population averages (*see* **Note 13**). This quantitative image-based cytometry approach allows for sensitive and reliable measurements of dynamic changes in PAR levels and DNA damage signaling in thousands of asynchronously growing cells in a cell cycle resolved manner (Figs. 1 and 2). Key advantages and limitations of this technique are discussed in Subheading 4 (*see* **Note 14**).

4 Notes

1. Most adherent cell lines that can be used for indirect immunofluorescence experiments are also suitable for quantitative image-based cytometry. Cells can be grown on glass coverslips as described here or on multi-well imaging plates. The optimal cell density should be chosen so that it is high enough to allow for a large number of cells being analyzed per image while avoiding contact between the nuclei of neighboring cells in order to facilitate software-assisted object detection (Fig. 1a). For most adherent cell lines, a cell density of 70–90% fulfills these criteria.
2. Testing different treatment durations can reveal the dynamics of cellular stress responses and provide clues to the underlying

molecular mechanisms. This is facilitated by the sensitivity of state-of-the-art microscope systems and the possibility to specifically focus on cell subpopulations by quantitative image-based cytometry. Here, we have used treatment durations between 5 and 60 min for oxidative stress treatments (Fig. 1b) and durations from 30 min to 4 h for PARP inhibitor treatments (Fig. 2a, b).

3. PAR induction during sample preparation has been reported [11, 24]. When exact PAR measurements or quantifications of basal PAR levels are critical, fixation conditions may have to be optimized, and PARP and PARG inhibitors may have to be added during the fixation step in order to minimize the risk of undesirable changes in intracellular PAR levels.

   It is recommended to continue with the staining immediately after the fixation or to store the fixed cells at 4 °C overnight and perform the staining on the next working day. In some cases, longer storage of fixed cells may be possible if unwanted effects on the staining quality can be ruled out. Prior to fixation, different pre-extraction protocols can be used to remove soluble protein fractions and focus the analysis on extraction-resistant protein pools [3, 21].

4. EdU incorporation combined with quantification of DNA content allows for two-dimensional image-based cell cycle staging (Fig. 1c) and has the advantage that the Click-iT reaction can be combined with a dual antibody staining. Two-dimensional image-based cell cycle staging can also be achieved by combining DAPI-based DNA content measurements with measurements of cyclin A levels, which rise as cells progress through S-phase and into G2 (Fig. 1d). Other endogenous cell cycle markers and fluorescent cell cycle reporters can also be used.

5. Primary antibody incubations may have to be optimized for every antibody. When using small volumes of antibody solution for extended periods of incubation time, precautions have to be taken to avoid evaporation. Using a wet chamber or sealing the plate with parafilm is recommended. Alternatively, coverslips can be incubated in primary antibody solution in 24-well plates using 250 μl antibody solution per well.

6. Depending on the experimental setup and the available imaging equipment, combinations of fluorophores can be chosen in a way that avoids bleed-through between the different color channels. Where this is not possible or in case of doubt, control experiments should be performed prior to extracting quantitative data.

7. DAPI concentration and incubation time may have to be optimized for different cell lines. Terminating the DNA staining by

removal of the DAPI solution followed by PBS washes facilitates quantitative image-based cell cycle staging. Accordingly, total DAPI intensities scale with DNA content and allow for a discrimination of the different cell cycle phases from 2 N to 4 N (Fig. 2a, b).

8. Although other mounting media can be used, Mowiol-based mounting medium polymerizes evenly and thereby facilities multi-position autofocus regimes during automated image acquisition. For Mowiol preparation mix 2.4 g Mowiol with 6.9 g of 86–89% glycerol. While stirring, add 6 ml distilled water and leave stirring for 2 h at room temperature. Add 12 ml of 0.2 M Tris (pH 8.5). Incubate at 50–60 °C for 10 min to resolve all components. Repeat if necessary until all components are dissolved. Prepare aliquots and store at −20 °C. Mounted coverslips can be stored overnight at 4 °C to allow for complete polymerization prior to image acquisition.
9. The number of images per condition depends on cell density, desired resolution and objective, camera field of view, and the amount of cells required for the experimental readout. It may range from a single image using a low magnification objective (4×) resulting in image information of more than 10.000 cells to a 10 × 10 image grid (100 images per condition), for instance, using a high magnification objective (40×) resulting in about 1000–5000 cells depending on cell density and field of view. Of note, even a moderate upscaling from one to ten high resolution images per condition (acquired in an automated manner or even manually) will result in image information of up to 500 cells and thus allow for an assessment of subpopulation-specific responses.
10. In addition to the Olympus ScanR system, we recently used a Leica DMI 6000 inverted microscope equipped with a motorized stage, a tri-band bandpass filter, and a 12-bit monochrome EMCCD camera (Leica DFC 350 FX 1392 × 1040 pixels, 6.4 μm pixel size) for similar analyses [23]. In principal, besides dedicated high-content platforms (e.g., Olympus ScanR, Thermo Scientific Cellomics ArrayScan, Molecular Devices ImageXpress Ultra/Micro, GE Healthcare IN Cell Analyzer 6000/2200, Perkin Elmer Opera/Operetta, BD Biosciences BD Pathway 855/435), any automated fluorescence microscope, wide-field or confocal, can be used. Even manually acquired images can be subjected to quantitative image-based cytometry analyses.
11. Here, we focused our analyses on mean and total nuclear intensities of DAPI, EdU, cyclin A, PAR, and γH2AX. Provided that suitable antibodies are available, other markers can be

measured in a very similar manner, and additional cellular parameters can be assessed through software-assisted image segmentation and feature extraction. With sufficient image resolution, also subcellular structures (e.g., DNA damage foci) can be segmented and quantified.

12. Various commercial software packages can be used for image segmentation and feature extraction. ImageJ [25], Fiji [26], CellCognition [27], and CellProfiler [28] are open-source alternatives.
13. The free software environment for statistical computing and graphics R can be used as an alternative for data visualization and analysis.
14. Here, we demonstrate how automated high-content imaging can be used to assess the dynamics of the cellular response to oxidative damage as well as to PARP inhibitor-induced genotoxicity in a cell cycle resolved manner. Such upscaling of conventional immunofluorescence experiments transforms single-cell imaging into a cell population assay that enables information-rich multidimensional readouts. This can reveal subpopulation-specific responses and combines the advantages of analyzing thousands of individual cells with the spatial resolution of high-end microscope lenses. Hence, this approach can provide detailed insights into the dynamics of PAR formation and DNA damage signaling in asynchronously growing cell populations. The described technology represents an important complementary approach to cell population average measurements by current proteomics, genomics, and transcriptomics approaches. As with any immunofluorescence-based method, limitations exist with regard to the number of different markers that can be combined in a single staining and the availability of suitable antibodies. Specifically, the antibody used to detect PAR is unlikely to recognize short oligomers of ADP-ribose, limiting the detection to polymers of ADP-ribose. Further, although sensitive, robust, and highly reliable, all measurements are relative quantifications and therefore primarily suited for relative comparisons of different treatment conditions. Moreover, while cells growing in suspension can be spun down and immobilized on imaging slides or imaging multi-well plates to allow for their analysis by quantitative image-based cytometry, cells growing in dense colonies or in spheres may require more elaborate adjustments. For most adherent cell types, however, the presented method has widespread applicability and the potential to lead to important new findings in the area of PARP biology and beyond.

Acknowledgments

We are grateful to our lab members Thomas Schmid, Federico Teloni, and Stefania Pellegrino for their help with quantitative image-based cytometry and to Jiri Lukas and Luis Toledo for sharing reagents and exchange of unpublished results. Luis Toledo also provided valuable comments on the manuscript. Urs Ziegler and José María Mateos Melero from the Center for Microscopy and Image Analysis at the University of Zurich are acknowledged for expert microscopy support. Research in the lab of Matthias Altmeyer is financed by the Swiss National Science Foundation (SNSF Professorship Grant PP00P3_150690) and by the University of Zurich Association Research Talent Development Fund.

References

1. Hottiger MO (2015) Nuclear ADP-ribosylation and its role in chromatin plasticity, cell differentiation, and epigenetics. Annu Rev Biochem 84:227–263. doi:10.1146/annurev-biochem-060614-034506
2. Teloni F, Altmeyer M (2016) Readers of poly(ADP-ribose): designed to be fit for purpose. Nucleic Acids Res 44(3):993–1006. doi:10.1093/nar/gkv1383
3. Altmeyer M, Neelsen KJ, Teloni F, Pozdnyakova I, Pellegrino S, Grofte M, Rask MB, Streicher W, Jungmichel S, Nielsen ML, Lukas J (2015) Liquid demixing of intrinsically disordered proteins is seeded by poly(ADP-ribose). Nat Commun 6:8088. doi:10.1038/ncomms9088
4. Aguzzi A, Altmeyer M (2016) Phase separation: linking cellular compartmentalization to disease. Trends Cell Biol. 26(7):547–558 doi:10.1016/j.tcb.2016.03.004
5. O'Connor MJ (2015) Targeting the DNA damage response in cancer. Mol Cell 60(4):547–560. doi:10.1016/j.molcel.2015.10.040
6. Lord CJ, Ashworth A (2016) BRCAness revisited. Nat Rev Cancer. 16(2):110–120. doi:10.1038/nrc.2015.21
7. Kraus WL (2015) PARPs and ADP-ribosylation: 50 years ... and counting. Mol Cell 58(6):902–910. doi:10.1016/j.molcel.2015.06.006
8. Gagne JP, Haince JF, Pic E, Poirier GG (2011) Affinity-based assays for the identification and quantitative evaluation of noncovalent poly(ADP-ribose)-binding proteins. Methods Mol Biol 780:93–115. doi:10.1007/978-1-61779-270-0_7
9. Gagne JP, Pic E, Isabelle M, Krietsch J, Ethier C, Paquet E, Kelly I, Boutin M, Moon KM, Foster LJ, Poirier GG (2012) Quantitative proteomics profiling of the poly(ADP-ribose)-related response to genotoxic stress. Nucleic Acids Res 40(16):7788–7805. doi:10.1093/nar/gks486
10. Isabelle M, Gagne JP, Gallouzi IE, Poirier GG (2012) Quantitative proteomics and dynamic imaging reveal that G3BP-mediated stress granule assembly is poly(ADP-ribose)-dependent following exposure to MNNG-induced DNA alkylation. J Cell Sci 125(Pt 19):4555–4566. doi:10.1242/jcs.106963
11. Jungmichel S, Rosenthal F, Altmeyer M, Lukas J, Hottiger MO, Nielsen ML (2013) Proteome-wide identification of poly(ADP-ribosyl)ation targets in different genotoxic stress responses. Mol Cell 52(2):272–285. doi:10.1016/j.molcel.2013.08.026
12. Rosenthal F, Hottiger MO (2014) Identification of ADP-ribosylated peptides and ADP-ribose acceptor sites. Front Biosci 19:1041–1056
13. Daniels CM, Ong SE, Leung AK (2015) The promise of proteomics for the study of ADP-ribosylation. Mol Cell 58(6):911–924. doi:10.1016/j.molcel.2015.06.012
14. Bartolomei G, Leutert M, Manzo M, Baubec T, Hottiger MO (2016) Analysis of chromatin ADP-ribosylation at the genome-wide level and at specific loci by ADPr-ChAP. Mol Cell 61(3):474–485. doi:10.1016/j.molcel.2015.12.025
15. Roukos V, Pegoraro G, Voss TC, Misteli T (2015) Cell cycle staging of individual cells by fluorescence microscopy. Nat Protoc 10(2):334–348. doi:10.1038/nprot.2015.016
16. Blasi T, Hennig H, Summers HD, Theis FJ, Cerveira J, Patterson JO, Davies D, Filby A, Carpenter AE, Rees P (2016) Label-free cell

cycle analysis for high-throughput imaging flow cytometry. Nat Commun 7:10256. doi:10.1038/ncomms10256

17. Boutros M, Heigwer F, Laufer C (2015) Microscopy-based high-content screening. Cell 163(6):1314–1325. doi:10.1016/j.cell.2015.11.007
18. Liberali P, Snijder B, Pelkmans L (2015) Single-cell and multivariate approaches in genetic perturbation screens. Nat Rev Genet 16(1):18–32. doi:10.1038/nrg3768
19. Sailem HZ, Cooper S, Bakal C (2016) Visualizing quantitative microscopy data: history and challenges. Crit Rev Biochem Mol Biol 51(2):96–101. doi:10.3109/10409238.2016.1146222
20. Altmeyer M, Toledo L, Gudjonsson T, Grofte M, Rask MB, Lukas C, Akimov V, Blagoev B, Bartek J, Lukas J (2013) The chromatin scaffold protein SAFB1 renders chromatin permissive for DNA damage signaling. Mol Cell 52(2):206–220. doi:10.1016/j.molcel.2013.08.025
21. Toledo LI, Altmeyer M, Rask MB, Lukas C, Larsen DH, Povlsen LK, Bekker-Jensen S, Mailand N, Bartek J, Lukas J (2013) ATR prohibits replication catastrophe by preventing global exhaustion of RPA. Cell 155(5):1088–1103. doi:10.1016/j.cell.2013.10.043
22. Larsen DH, Hari F, Clapperton JA, Gwerder M, Gutsche K, Altmeyer M, Jungmichel S, Toledo LI, Fink D, Rask MB, Grofte M, Lukas C, Nielsen ML, Smerdon SJ, Lukas J, Stucki M (2014) The NBS1-treacle complex controls ribosomal RNA transcription in response to DNA damage. Nat Cell Biol 16(8):792–803. doi:10.1038/ncb3007
23. Ahuja AK, Jodkowska K, Teloni F, Bizard AH, Zellweger R, Herrador R, Ortega S, Hickson ID, Altmeyer M, Mendez J, Lopes M (2016) A short G1 phase imposes constitutive replication stress and fork remodelling in mouse embryonic stem cells. Nat Commun 7:10660. doi:10.1038/ncomms10660
24. Beneke S, Meyer K, Holtz A, Huttner K, Burkle A (2012) Chromatin composition is changed by poly(ADP-ribosyl)ation during chromatin immunoprecipitation. PLoS One 7(3):e32914. doi:10.1371/journal.pone.0032914
25. Schneider CA, Rasband WS, Eliceiri KW (2012) NIH image to ImageJ: 25 years of image analysis. Nat Methods 9(7):671–675
26. Schindelin J, Arganda-Carreras I, Frise E, Kaynig V, Longair M, Pietzsch T, Preibisch S, Rueden C, Saalfeld S, Schmid B, Tinevez JY, White DJ, Hartenstein V, Eliceiri K, Tomancak P, Cardona A (2012) Fiji: an open-source platform for biological-image analysis. Nat Methods 9(7):676–682. doi:10.1038/Nmeth.2019
27. Held M, Schmitz MHA, Fischer B, Walter T, Neumann B, Olma MH, Peter M, Ellenberg J, Gerlich DW (2010) CellCognition: time-resolved phenotype annotation in high-throughput live cell imaging. Nat Methods 7(9):747–U118. doi:10.1038/nmeth.1486
28. Carpenter AE, Jones TR, Lamprecht MR, Clarke C, Kang IH, Friman O, Guertin DA, Chang JH, Lindquist RA, Moffat J, Golland P, Sabatini DM (2006) CellProfiler: image analysis software for identifying and quantifying cell phenotypes. Genome Biol 7(10):R100. doi:10.1186/gb-2006-7-10-r100